

STRUCTURAL EVOLUTION AND OPTICAL PROPERTIES OF TiO₂ THIN FILMS PREPARED BY THERMAL OXIDATION OF PLD Ti FILMS

D. Luca^{a*}, L. S. Hsu

Department of Physics, National Chang-Hua University of Education, Chang-Hua 50058,
Taiwan, Republic of China

TiO₂ thin films have been prepared by thermal oxidation of Ti thin films grown on crystalline substrates (Si, SiO₂, and LaAlO₃) by pulsed-laser deposition. The specimens were *ex situ* post-annealed under 1 atm oxygen, between 600 and 1000 °C. The surface morphology, film composition, and structure were evaluated from SEM, EDX, XPS, XRD, and Raman data. Wavelength dependence of the refractive index and absorption coefficient in the UV-VIS-near IR regions, as well as the optical band gap were inferred from optical transmittance measurements. The characteristics of the investigated thin films are interpreted in terms of amorphous-crystalline phase transitions and the role of oxygen defects.

(Received June 26, 2003; accepted August 21, 2003)

Keywords: Titanium dioxide, Pulsed-laser deposition, Thermal oxidation, Phase transition, Raman shift, Optical band gap

1. Introduction

TiO₂ has been a subject of intensive research due to its outstanding physical and chemical characteristics. During last decade, basic and applied research focused on the preparation and characterization of TiO₂ thin films, which feature large energy gap, excellent visible and near-IR transmittance, high refractive index (2.75 at 550 nm) and dielectric constant ($\epsilon_r \sim 170$). It was found that TiO₂ is antibacterial, self-cleaning, super-hydrophilic, and able to decompose organic substances. Various other applications of TiO₂ thin films are encountered in electronics, optics, environment protection, and medicine [1-4]. Only *anatase* and *rutile* TiO₂ phases both of tetragonal structure have been identified in thin films. The crystal structure of TiO₂ can be described as two chains of differently distorted TiO₆ octahedra. The differences in assembly patterns within the chains and in the lattice structures result in different band structure and band gap of the two phases (3.20 eV for anatase and 3.05 eV for rutile [5]). Due to larger band gap and lower electron-hole recombination probability, the anatase phase is more active in photo catalysis than the rutile phase. Much effort has been paid for the growth of anatase TiO₂ thin films with enhanced photocatalytic activity. Recently, thermally stable and highly crystalline anatase thin films have been prepared at temperatures as high as 1000 °C using (100) SrTiO₃ (STO) as substrate. LaAlO₃ (LAO) might be a better substrate for growing anatase TiO₂ thin films, since its lattice constant matches that of anatase within 0.1%. On the other hand, the lattice mismatch between rutile and the LAO substrate is higher than 15% [6]. Several preparation methods for TiO₂ thin films are described in the literature, such as ion-assisted techniques [7], pulsed-laser deposition (PLD) [5], and thermal oxidation of Ti or TiN surface [8,9]. Doped and undoped TiO₂ films prepared by reactive rf sputtering were also prepared and investigated [10].

Results are presented in this work concerning the preparation of TiO₂ thin films by thermal oxidation of Ti thin films grown by PLD. Surface morphology, film structure and composition were

^a On leave from the Faculty of Physics, Al. I. Cuza University, Iasi, Romania

* Corresponding author: dluca@cc.ncue.edu.tw

evaluated using SEM, EDX, XRD and Raman techniques. The wavelength dependence of the refractive index and optical absorption coefficient of the TiO₂ films in the UV-VIS-NIR range, as well as the value of the band gap have been inferred from the optical transmittance data. The results were interpreted in terms of the role of the oxygen defects and structural evolution during amorphous-crystalline phase transitions. In the paper [11] is reported the annealing effect on the PLD TiO₂ thin films.

2. Experimental details

Deposition of the Ti thin films was done in a high-vacuum chamber, which was evacuated to a base pressure of 1×10^{-6} Torr by means of a turbo-molecular pump (Fig. 1). The gas pressure inside the PLD chamber was measured using a cold cathode gauge and adjusted via an electronic mass flow controller. The gas sampling system used the Stanford Research Systems SRS – RGA 200 residual gas analyzer, as a core part. The residual oxygen partial pressure inside the PLD chamber was less than 4×10^{-7} Torr. According to previous X-ray photoelectron spectroscopy (XPS) measurements, the characteristic oxidation time under this oxygen pressure is about 500 s [9], which is larger than our total deposition time. Therefore, oxygen content in the PLD Ti thin films remained low.

The laser ablation of the Ti target (99.5% purity) was performed using the laser beam produced by a KrF excimer laser ($\lambda = 248$ nm, 20 ns pulse duration, 10 Hz repetition rate) model Lambda Physik, COMPex 102. The laser beam was focused on a 3.5×0.5 mm² area of the ablated target, at an incident angle of 45°. To diminish the occurrence of Ti drops, which might be splashed out from the metallic targets during laser ablation, the process was done under an inert gas atmosphere (1×10^{-3} mbar Ar gas). Laser pulse energy was chosen below the splashing threshold of metallic Ti [12]. The ablation spot was permanently rastered on the Ti target surface to ablate fresh material and avoid the effects of target cratering.

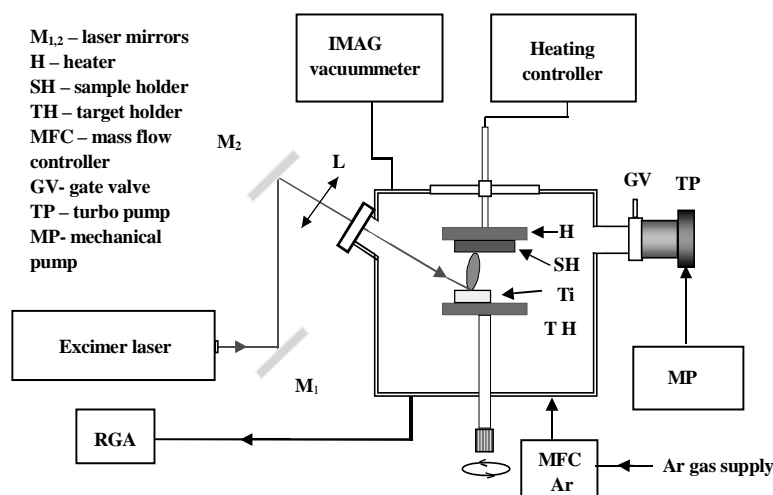


Fig. 1. The schematic of the PLD system.

The substrate temperature during deposition was 120 °C. Before deposition, the substrates were sonicated for 15 min in acetone, then rinsed and soaked. The Ti thin films were deposited onto (100) Si, (100) SiO₂, and (100) LAO single crystal substrates, using 6000 laser shots, each with energy of 100 mJ. In all the reported experiments the target-to-substrate distance was 5 cm. Sequential *ex situ* post deposition thermal oxidation was performed at 600, 650, 750 and 1000 °C, for 1 h, under the conditions of rapid heating up and cooling down rates (15 °C/min).

The film structure was determined by X-ray diffraction using the SCINTAG DMS 2000 XRD

equipment in a θ - 2θ configuration, using the Fe K α radiation ($\lambda = 1.93604 \text{ \AA}$). Complementary information concerning film microstructure was derived from Raman spectra, which were acquired by means of a SPEX 1403 0.85 m double spectrometer, using the blue line (488 nm) of an Ar⁺ laser as excitation source. Film morphology and composition were evaluated from XPS and EDX measurements performed on a Hitachi S3000N scanning electron microscope, equipped with a Horiba electron microprobe. The XPS measurements were done using an Mg K α X-ray source (1253.4 eV) and a detection angle of 45° with respect to the surface normal.

Spectral measurements have been performed using an UV/VIS/near-IR spectrophotometer (JASCO-V570). The optical transmittance of the samples deposited onto polished transparent SiO₂ substrates was monitored in the range 250–2000 nm. From the optical transmittance spectra, the wavelength dependence of the refractive index and optical absorption coefficient was inferred using the transmittance envelope method [13]. The optical band gap for the TiO₂ thin films (ΔE_g) was calculated from $(\alpha hv)^{1/2}$ vs. $h\nu$ plots [8].

3. Results and discussion

3.1. Film morphology and composition

As shown in Fig. 2, the Ti thin films feature a smooth surface on the nanometer scale, with no grain boundaries and few sub micron droplets. The occurrence of these few Ti droplets is the result of incomplete elimination of target splashing during laser ablation, in spite of precautions mentioned in Sec. 2. High repetition rate of the laser pulses, which is required to assure high deposition rate and low oxygen contamination of the PLD Ti film, may cause droplets and cluster aggregates occur during ablation. We found that 10 Hz is an optimum repetition rate for growing good quality Ti thin films.

Fig. 3 shows the EDX spectrum of a Ti thin film deposited on a Si substrate. The Ti peaks appear along with a large Si substrate peak. A very small C peak and no oxygen signal were detected in the EDX spectrum, which demonstrates that the thin film is essentially clean Ti. Similar results were found for Ti thin films deposited on SiO₂ and LAO, except for the presence of oxygen signal from the substrate. The evolution of the oxygen peak in the EDX spectra showed a gradual increase of the oxygen signal, until the saturation state was reached, after thermal oxidation at 750 °C.



Fig. 2. A surface SEM image of a PLD Ti thin film grown on Si.

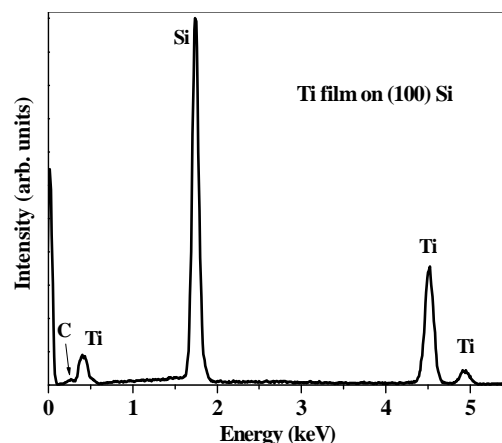


Fig. 3. The EDX spectrum of a Ti thin film grown on Si.

XPS was used to determine the surface composition of our thin films. The deconvolution of the Ti 2p and O 1s peaks in the XPS spectra was done by a software package [14] assuming a Shirley-type baseline and a Gaussian-Lorentzian peak. The following binding energies were used for the different oxidation states of titanium: Ti⁰ at 454.1 eV; Ti²⁺ at 455.1 eV; Ti³⁺ at 457.2 eV; and Ti⁴⁺ at 459.2 eV [15]. The atomic concentration ratio O/Ti was calculated from the integral peak area of

O 1s and Ti 2p peaks after taking into account the photo-ionization cross sections and the transmission function of the spectrometer.

As seen in Fig. 4, a decrease of the intensity of the Ti⁰ state occurs after successive thermal oxidation at 650 and 750 °C. Unlike previously reported [4,16], Ti²⁺ and Ti³⁺ states are present in the films oxidized at 600 and 650 °C, but practically absent in our XPS spectra of the films oxidized at 750 °C. It was reported that during thermal oxidation under 10⁻³-10⁻⁵ mTorr O₂, titanium suboxides develop in deeper layers of the Ti surface, while TiO₂ occurs in the top layers [15]. During further oxidation, TiO₂ gradually substitutes the titanium suboxides. The substitution kinetics is dependent on both O₂ gas pressure and oxidation temperature. Since thermal oxidation of our films at 750 °C was done under 1 atm O₂ for 1 h, it finally resulted in essentially TiO₂ thin films.

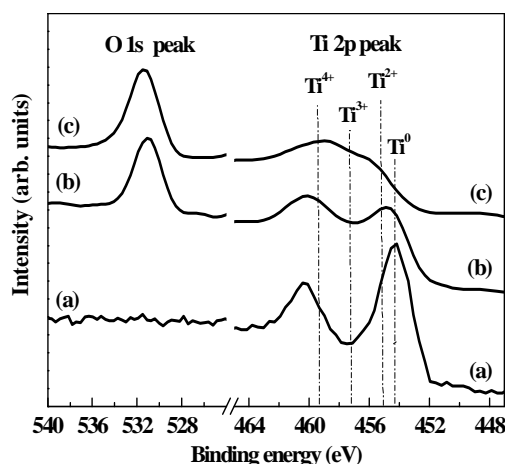


Fig. 4. O 1s and Ti 2p XPS spectra of (a) a clean Ti surface, and after annealing at (b) 600 °C and (c) 750 °C.

XPS measurements show that the thin films oxidized at 750 °C have saturation values of the O/Ti ratio between 1.95 and 2.01. The symmetrical shape of the O 1s XPS peak is an additional indication that our films are essentially TiO₂.

The XPS spectrum of the Ti surface after thermal oxidation at 750° showed approximately 4% carbon contamination on the Ti surface. This is caused by the extreme reactivity of titanium for hydrocarbons, which are usually present in the residual gas of the preparation chamber.

3.2. Film structure

Fig. 5 shows the XRD patterns of an as-deposited Ti thin film and of the same film after successive oxidation at temperatures between 650 and 1000 °C. The XRD pattern of an anatase-rutile TiO₂ sintered pellet is also displayed. The XRD patterns show that the as-deposited sample is amorphous Ti. A small (101) TiO₂ anatase peak occurs after thermal oxidation at 650 °C, while no rutile peak is present. We also note that no higher-index anatase peaks are observed. This observation contradicts the previous results concerning the occurrence of only rutile phase after oxidation of thermally evaporated Ti films on quartz [9]. Subsequent thermal oxidation at 750 °C (Fig. 5) results in an increase of the anatase (101) peak intensity and a gradual shift towards lower angles. This shift is a consequence of the enlargement of lattice volume due to incorporation of oxygen atoms in the film during thermal oxidation. After oxidation at 1000 °C, a significant decrease of the (101) anatase peak intensity and a large (110) rutile peak occur. For comparison, in sputtered TiO₂ thin films an anatase-rutile phase mixture occurs when they are deposited at temperatures below 500 °C [9]. Unfortunately, XRD cannot be used to monitor the (101) anatase peak for films deposited on LAO, due to its overlapping with a large LAO peak. Therefore, Raman scattering was chosen to monitor the phase composition of the TiO₂ deposited on this substrate. Raman scattering is able to probe the film

microstructure within a volume of a few unit cells and provides additional information concerning nano-crystallite size and lattice imperfections.

Fig. 6 shows the Raman spectra of the TiO₂ thin film on a LAO substrate, prepared by thermal oxidation of a Ti film at 600 °C and 650 °C. A clearly defined anatase E_{1g} Raman peak occurs at 143.9 cm⁻¹ after the oxidation at 600 °C. Further annealing at 650 °C in oxygen results in an increase of the peak intensity, a decrease of the peak width, and a slight blue shift (0.8 eV). The reduction in the peak width of the E_{1g} main anatase Raman mode is a result of the increase in crystallite size after oxidation through the mechanism of phonon confinement, as reported for TiO₂ anatase thin films prepared by chemical process. The blue shift of the Raman peak occurs as a consequence of the presence of sub-oxides in the first stage of thermal oxidation of the Ti thin films, as evidenced by both EDX and XPS.

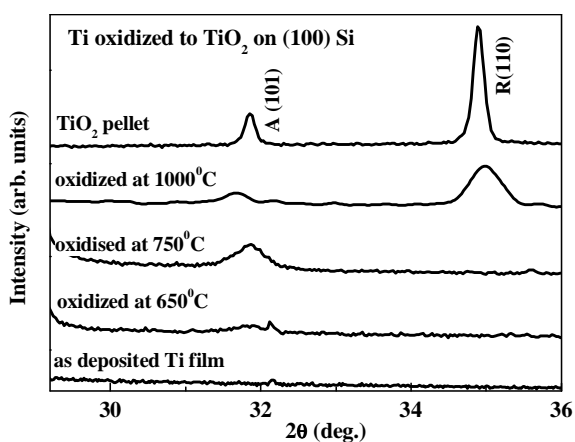


Fig. 5. XRD patterns of the as-deposited Ti thin film on Si, and after oxidizing at 650, 750, and 1000 °C.

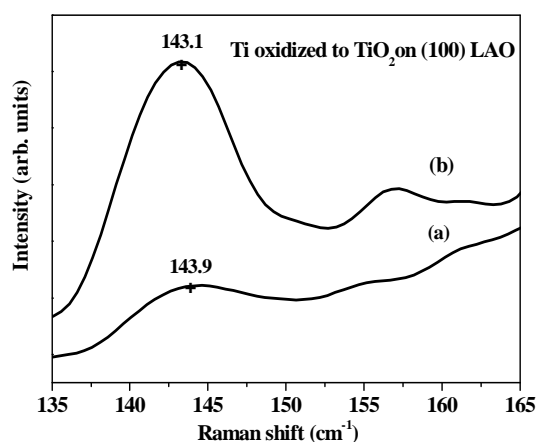


Fig. 6. Raman spectra of a Ti thin film grown on LAO after oxidizing under 1 atm O₂ for 1 h at (a) 600 °C and (b) 650 °C.

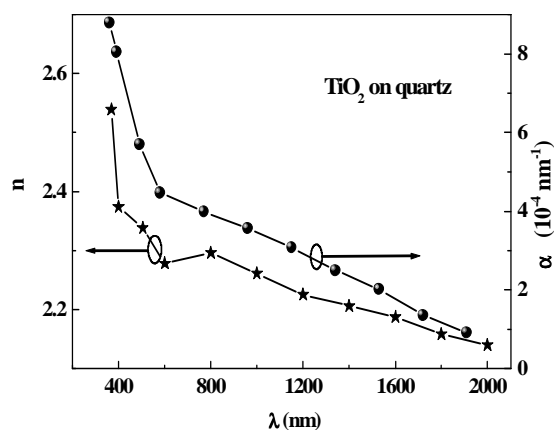


Fig. 7. Wavelength dependence of the refractive index n and the absorption coefficient α of a TiO₂ thin film on quartz, after oxidation at 650 °C.

3.3. Optical properties

Progressive thermal oxidation leads to an increase of film transmittance in the 300–2000 nm wavelength range. The visual aspect of the thin films changes from half-transparent dark gray to fully transparent after the first oxidation at 600 °C and remains unchanged even after oxidation at 1000 °C. The increase in the overall optical transmittance was previously observed for anatase TiO₂ crystalline thin films [7] and was ascribed to the decrease of oxygen vacancy concentration in the thin films by thermal

oxidation. This is in agreement with our EDX and XPS data, which indicate the increase of the oxygen content after oxidizing in 1 atm O₂.

The optical transmittance data of the TiO₂ thin films were used to calculate the wavelength dependence of the refractive index (n) and the absorption coefficient (α) [12]. The results are presented in Fig. 7 for a TiO₂ thin film grown on quartz. The n value decreases from a maximum value of 2.54 at 400 nm to below 2.2 in the near infrared range. These are typical n values for the anatase TiO₂ phase [9]. A rapid decrease of the α value takes place in the range UV range, followed by a linear decrease in the visible and near-infrared range. Other measurements showed that further increase in oxidation temperature and time leads to an increase in n and essentially constant α . This is a result of the occurrence of an increasing amount of rutile phase, which is characterized by a higher compactness and concentration of oxygen defects [9]. The optical band gap decreased from 3.18 eV to 3.10 eV when the oxidation temperature increased from 750 to 1000 °C. Similar results have been found for TiO₂ thin films prepared by thermal oxidation of thermally evaporated Ti films, which were ascribed to electronic disorder due to oxygen nonstoichiometry developed at temperatures around 1000 °C [9].

4. Conclusions

We investigated the morphological, structural, and optical properties of anatase TiO₂ thin films prepared by thermal oxidation of Ti thin films, which were grown by PLD on various crystalline substrates at 120 °C under an Ar gas pressure of 1 mTorr. After oxidizing the Ti thin films at 600 °C, a pure anatase phase appeared on the LAO substrate, while a mixture of amorphous and anatase phases appeared on the Si and SiO₂ substrates. For the films grown on LAO, the occurrence of the anatase phase after thermal oxidation at temperatures as low as 600 °C is due to the good lattice match between the film and the substrate.

Highly crystalline TiO₂ anatase thin films can also be prepared by thermal oxidation of PLD grown Ti films on quartz or Si, provided that subsequent oxidation is done at higher temperatures and longer duration (at 650 and 750 °C for 1 h each). The thermal oxidation at temperatures below 1000 °C results in good-quality pure crystalline TiO₂ anatase thin films. Oxidation above 1000 °C leads to the occurrence of the rutile phase, which has higher refractive index and lower energy gap than the anatase phase.

Acknowledgements

We thank C. J. Liu for help in oxidation the samples, and Y.-T. Lee and Y. C. Chi for Raman and SEM measurements, respectively. This work is sponsored by National Science Council, Taiwan, Republic of China under Grants NSC91-2112-M-018-007 and NSC 92-2811-M-018-001.

References

- [1] Y. H. Lee, K.K. Chan, M. J. Brady, *J. Vac. Sci. Technol.* **A13**, 596 (1995).
- [2] T. Nakayama, K. Onisawa, M. Fuyama, K. Hanazono, *J. Electrochem. Soc.* **139**, 1204 (1992).
- [3] K. Jurek, M. Guglielmi, G. Kuncova, O. Renner, F. Lukes, M. Navratil, E. Krouscky, V. Vorlicek, K. Kokesova, *J. Mater. Sci.* **27**, 2549 (1992).
- [4] F. Zhang, X. Liu, Y. Mao, N. Huang, Y. Chen, Z. Zheng, and Z. Zhou, A. Chen, and Z. Jiang, *Surf. Coat. Technol.* **103-104**, 146 (1998).
- [5] A. K. Sharma, R. K. Tareja, U. Wilker, and W. Schade, *Appl. Surf. Sci.* **206**, 137 (2003).
- [6] C. K. Ong, S. J. Wang, *Appl. Surf. Sci.* **185**, 47 (2001).
- [7] Y. Yamada, H. Uyama, T. Murata, H. Nozoye, *J. Vac. Sci. Technol. A* **19**, 2479 (2001).
- [8] C. C. Ting, S. Y. Chen, *J. Appl. Phys.* **88**, 4628 (2000).
- [9] D. Luca, A. W. D. van der Gon, M. W. G. Ponjée, G. Popa, L.S. Hsu (unpublished results).
- [10] D. Mardare, G. I. Rusu, *J. Optoelectron. Adv. Mater.* **3**(1), 95 (2001).
- [11] L. S. Hsu, D. Luca, *J. Optoelectron. Adv. Mater.* **5**(4), 791 (2003)
- [12] L. C. Chen, *Pulsed Laser Deposition of Thin Films*, D. B. Chrisey, G. K. Hubler (eds), John Wiley, NY, 1994, p. 190.
- [13] R. Swanepoel, *J. Phys E: Sci. Instrum.* **16**, 1214 (1983).
- [14] R. W. M. Kwok, *XPSPEAK v.4.1 Manual*, Hong Kong, 1991.
- [15] G. Lu, S. L. Bernasek, *J. Schwartz: Surf. Sci.* **458**, 80 (2000).
- [16] W. F. Zhang, Y. L. He, M. S. Zhang, Z. Yin, Q. Chen, *J. Phys. D: Appl. Phys.* **33**, 912 (2000).